

CURRENT CLINICAL IMAGING • RICHARD C. SEMELKA, SERIES EDITOR

WOMEN'S IMAGING

MRI with Multimodality Correlation

EDITED BY

MICHELE A. BROWN

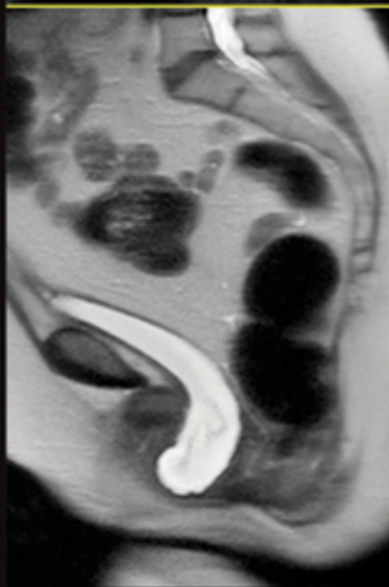
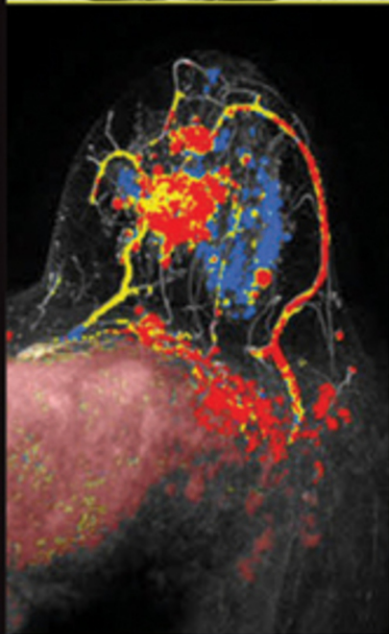
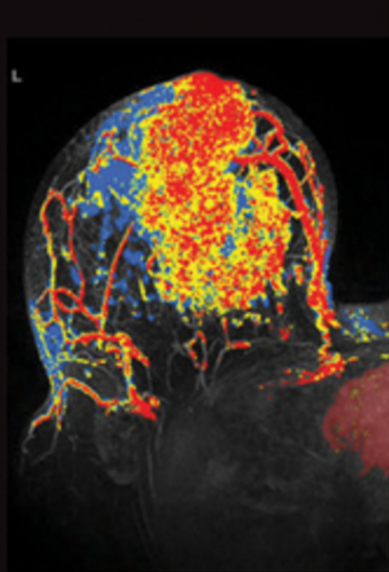
HAYDEE OJEDA-FOURNIER

DRAGANA DJILAS

MOHAMED EL-AZZAZI

RICHARD C. SEMELKA

WILEY Blackwell



Women's Imaging

Women's Imaging MRI with Multimodality Correlation

Edited by

Michele A. Brown, MD

Professor of Clinical Radiology
UC San Diego Health System
San Diego, CA, USA

Haydee Ojeda-Fournier, MD

Associate Professor of Clinical Radiology
Medical Director, Breast Imaging Section
Director Medical Student Education in Radiology
Moore's Cancer Center
UC San Diego Health System
La Jolla, CA, USA

Dragana Djilas, MD, PhD

Associate Professor of Radiology
Center for Diagnostic Imaging
Oncology Institute of Vojvodina
Novi Sad, Serbia

Mohamed El-Azzazi, MD, PhD

Clinical Research Scholar, MRI Section, Department of Radiology
University of North Carolina, Chapel Hill, NC, USA;
Professor of Radiology, Al-Azhar University
Cairo, Egypt;
Associate Professor of Radiology
Dammam University, Saudi Arabia; *and*
Consultant in Radiology
King Fahad University Hospital, Saudi Arabia

Richard C. Semelka, MD

Director, Magnetic Resonance Services;
Professor, Vice Chairman of Clinical Research; *and*
Vice Chairman of Quality and Safety
Department of Radiology
University of North Carolina at Chapel Hill
Chapel Hill, NC, USA

WILEY Blackwell

Copyright © 2014 by John Wiley & Sons, Inc. All rights reserved

Published by John Wiley & Sons, Inc., Hoboken, New Jersey
Published simultaneously in Canada

No part of this publication may be reproduced, stored in a retrieval system, or transmitted in any form or by any means, electronic, mechanical, photocopying, recording, scanning, or otherwise, except as permitted under Section 107 or 108 of the 1976 United States Copyright Act, without either the prior written permission of the Publisher, or authorization through payment of the appropriate per-copy fee to the Copyright Clearance Center, Inc., 222 Rosewood Drive, Danvers, MA 01923, (978) 750-8400, fax (978) 750-4470, or on the web at www.copyright.com. Requests to the Publisher for permission should be addressed to the Permissions Department, John Wiley & Sons, Inc., 111 River Street, Hoboken, NJ 07030, (201) 748-6011, fax (201) 748-6008, or online at <http://www.wiley.com/go/permissions>.

The contents of this work are intended to further general scientific research, understanding, and discussion only and are not intended and should not be relied upon as recommending or promoting a specific method, diagnosis, or treatment by health science practitioners for any particular patient. The publisher and the author make no representations or warranties with respect to the accuracy or completeness of the contents of this work and specifically disclaim all warranties, including without limitation any implied warranties of fitness for a particular purpose. In view of ongoing research, equipment modifications, changes in governmental regulations, and the constant flow of information relating to the use of medicines, equipment, and devices, the reader is urged to review and evaluate the information provided in the package insert or instructions for each medicine, equipment, or device for, among other things, any changes in the instructions or indication of usage and for added warnings and precautions. Readers should consult with a specialist where appropriate. The fact that an organization or Website is referred to in this work as a citation and/or a potential source of further information does not mean that the author or the publisher endorses the information the organization or Website may provide or recommendations it may make. Further, readers should be aware that Internet Websites listed in this work may have changed or disappeared between when this work was written and when it is read. No warranty may be created or extended by any promotional statements for this work. Neither the publisher nor the author shall be liable for any damages arising herefrom.

For general information on our other products and services or for technical support, please contact our Customer Care Department within the United States at (800) 762-2974, outside the United States at (317) 572-3993 or fax (317) 572-4002.

Wiley also publishes its books in a variety of electronic formats. Some content that appears in print may not be available in electronic formats. For more information about Wiley products, visit our web site at www.wiley.com.

Library of Congress Cataloging-in-Publication Data:

Women's imaging : MRI with multimodality correlation / edited by Michele A. Brown, Haydee Ojeda-Fournier, Dragana Djilas, Mohamed El-Azzazi, Richard C. Semelka.

p. ; cm.

Includes bibliographical references and index.

ISBN 978-1-118-48284-1 (cloth)

I. Brown, Michele A., editor of compilation. II. Ojeda-Fournier, Haydee, editor of compilation. III. Djilas, Dragana, editor of compilation. IV. El-Azzazi, Mohamed, editor of compilation. V. Semelka, Richard C., editor of compilation.

[DNLM: 1. Magnetic Resonance Imaging--methods. 2. Women's Health. WN 185]

RC386.6.M34

616.07'548--dc23

2013042717

Cover design by Wiley

Printed in the United States of America

10 9 8 7 6 5 4 3 2 1

Contents

Contributors, vii

Preface, ix

- 1 Pelvis MRI: introduction and technique, 1**
Michele A. Brown & Richard C. Semelka
- 2 Imaging the vagina and urethra, 8**
Shannon St. Clair, Randy Fanous, Mohamed El-Azzazi, Richard C. Semelka, & Michele A. Brown
- 3 Pelvic floor imaging, 27**
Laura E. Rueff & Steven S. Raman
- 4 Imaging the uterus, 49**
Randy Fanous, Katherine M. Richman, Chayanin Angthong, Mohamed El-Azzazi, & Michele A. Brown
- 5 Imaging the adnexa, 88**
Michele A. Brown, Mary K. O'Boyle, Chayanin Angthong, Mohamed El-Azzazi, & Richard C. Semelka
- 6 Imaging maternal conditions in pregnancy, 131**
Lorene E. Romine, Randy Fanous, Michael J. Gabe, Richard C. Semelka, & Michele A. Brown
- 7 Fetal imaging, 180**
Lorene E. Romine, Ryan C. Rockhill, Michael J. Gabe, Reena Malhotra, Richard C. Semelka, & Michele A. Brown
- 8 Breast MRI: introduction and technique, 239**
Michael J. Gabe, Jasmina Boban, Dragana Djilas, Vladimir Ivanovic, & Haydee Ojeda-Fournier
- 9 ACR breast MRI lexicon and interpretation, 264**
Julie Bykowski, Natasa Prvulovic Bunovic, Dragana Djilas, & Haydee Ojeda-Fournier
- 10 Preoperative breast cancer evaluation and advanced breast cancer imaging, 296**
Jade de Guzman, Dragana Bogdanovic-Stojanovic, Dragana Djilas, & Haydee Ojeda-Fournier
- 11 Postsurgical breast and implant imaging, 322**
Julie Bykowski, Dag Pavic, Dragana Djilas, & Haydee Ojeda-Fournier
- 12 MR-guided breast interventions, 346**
Michael J. Gabe, Dragana Djilas, Dag Pavic, & Haydee Ojeda-Fournier

Index, 363

Contributors

Chayanin Anghong, MD

Department of Radiology
University of North Carolina at Chapel Hill
Chapel Hill, NC, USA

Jasmina Boban, MD

Center for Diagnostic Imaging
Oncology Institute of Vojvodina
Novi Sad, Serbia

Dragana Bogdanovic-Stojanovic, MD, PhD

Assistant Professor of Radiology
Center for Diagnostic Imaging
Oncology Institute of Vojvodina
Novi Sad, Serbia

Michele A. Brown, MD

Professor of Clinical Radiology
UC San Diego Health System
San Diego, CA, USA

Julie Bykowski, MD

Assistant Professor of Clinical Radiology
Moores Cancer Center
UC San Diego Health System
La Jolla, CA, USA

Jade de Guzman, MD

Assistant Professor of Clinical Radiology
Moores Cancer Center
UC San Diego Health System
La Jolla, CA, USA

Dragana Djilas, MD, PhD

Associate Professor of Radiology
Center for Diagnostic Imaging
Oncology Institute of Vojvodina
Novi Sad, Serbia

Mohamed El-Azzazi MD, PhD

Clinical Research Scholar, MRI Section, Department of
Radiology
University of North Carolina, Chapel Hill, NC, USA;
Professor of Radiology, Al-Azhar University
Cairo, Egypt;
Associate Professor of Radiology
Dammam University, Saudi Arabia;
Consultant in Radiology
King Fahad University Hospital, Saudi Arabia

Randy Fanous, MD, BHSc

Department of Radiology
UC San Diego Health System
San Diego, CA, USA

Michael J. Gabe, MD

Department of Radiology
UC San Diego Health System
San Diego, CA, USA

Vladimir Ivanovic, BSCEE

Center for Diagnostic Imaging
Oncology Institute of Vojvodina
Novi Sad, Serbia

Reena Malhotra

Department of Radiology
North Shore-LIJ Health System
New Hyde Park, NY, USA

Mary K. O'Boyle, MD

Clinical Professor of Radiology
Chief of Ultrasound
UC San Diego Health System
San Diego, CA, USA

Haydee Ojeda-Fournier, MD

Associate Professor of Clinical Radiology
Medical Director, Breast Imaging Section
Director Medical Student Education in Radiology
Moore's Cancer Center
UC San Diego Health System
La Jolla, CA, USA

Dag Pavic, MD

Associate Professor of Radiology
Department of Radiology
Medical University of South Carolina
Charleston, SC, USA

Natasa Prvulovic Bunovic, MD

Consultant in Radiology
Center for Diagnostic Imaging
Oncology Institute of Vojvodina
Novi Sad, Serbia

Steven S. Raman, MD

Professor of Radiology, Surgery and Urology
David Geffen School of Medicine at UCLA
Los Angeles, CA, USA

Katherine M. Richman, MD

Clinical Professor of Radiology
UC San Diego Health System
La Jolla, CA, USA

Ryan C. Rockhill, MD

Body and Breast Imaging
Naval Medical Center San Diego
San Diego, CA, USA

Lorene E. Romine, MD

Assistant Clinical Professor of Radiology
UC San Diego Health System
San Diego, CA, USA

Laura E. Rueff, MD, MPH

Department of Radiology
University of California Los Angeles
Los Angeles, CA, USA

Richard C. Semelka, MD

Director, Magnetic Resonance Services
Professor, Vice Chairman of Clinical Research and
Vice Chairman of Quality and Safety
Department of Radiology
University of North Carolina at Chapel Hill
Chapel Hill, NC, USA

Shannon St Clair, MD

Department of Radiology
UC San Diego Health System
San Diego, CA, USA

Preface

Women's health issues consume a large portion of medical resources and healthcare dollars. Proper management requires a team of physicians from various specialties. Within the field of Radiology, there has been a trend toward developing a subspecialty dedicated to comprehensive imaging of women's healthcare needs, including gynecological, obstetric, genitourinary, and breast conditions. The term "Women's Imaging" is used differently in different contexts; for the purpose of this textbook, the term is used to describe imaging of the female reproductive system, including the pelvis and breast. An effective women's imager must work closely with clinical colleagues of various specialties and maintain a current understanding of diagnostic strategies, clinical implications of imaging findings, and the appropriate use of imaging tests to detect and monitor treatment.

The use of magnetic resonance imaging (MRI) for evaluation of gynecological, obstetric, and breast conditions has increased in recent years. MRI provides excellent tissue contrast resolution in the female pelvis and breast without ionizing radiation. Used together with complementary modalities, such as ultrasound and mammography, MRI has been shown to add important information to help guide patient care. The current text aims to provide the essentials of MRI in Women's Imaging, including indications, technique, and interpretation. For a number of entities, we illustrate the companion imaging studies of computed tomography, ultrasound, or mammography.

Hopefully this text serves to redress the considerable underutilization of MRI in these settings. Used appropriately, MRI is cost-effective and singularly informative. There are other textbooks on the separate topics of pelvic and breast MRI; the goal of this text is to combine and update the essentials of Women's Imaging MRI into a comprehensive and succinct overview.

The present volume is separated into two main sections: female pelvis (chapters 1–7) and breast (chapters 8–12). The first chapter presents current common indications and sample protocols for female pelvis MRI. Chapters 2–5 address pathology and respective imaging findings of the vagina and female urethra, pelvic floor, uterus, and adnexa. Chapters 6 and 7 focus on issues specific to pregnancy. Chapter 8 discusses rationale and technique for MRI of the breast. Chapters 9–12 are dedicated to the imaging features of breast disease and the role of MRI-guided intervention in the care of women with abnormal breast imaging findings.

This text is the collective effort of many individuals. I would like to thank the co-editors and contributors for their hard work. In addition, I am indebted to my radiology colleagues at the University of California San Diego for their help and support, with special thanks to every member of the body imaging and breast imaging divisions.

Michele A. Brown, MD

Chapter 1

Pelvis MRI: introduction and technique

Michele A. Brown & Richard C. Semelka

Imaging evaluation of the female pelvis

- Imaging plays an important role in the management of gynecological disease
- Ultrasound is often the initial imaging test
- Poor tissue contrast of CT limits gynecologic applications
- MRI benefits from excellent tissue contrast and lack of ionizing radiation
- Increased experience and availability have led to increased role of MRI
- MRI deemed appropriate by American College of Radiology for gynecological conditions, especially pre-treatment assessment of endometrial and cervical cancer, work-up of suspected adnexal mass, and evaluation of acute pelvic pain in reproductive-aged women in the setting of indeterminate ultrasound [1–4]
- Numerous gynecological and obstetric conditions are depicted by MRI, which may provide initial imaging (e.g., suspected urethral diverticulum) or problem-solving after ultrasound

Indications for MRI

(Table 1.1)

• Benign uterine conditions

- Anomalies
 - MRI considered imaging modality of choice
 - Informs management decisions (e.g., septate versus bicornuate uterus)
- Acquired disease
 - Problem solving for indeterminate ultrasound
 - MRI allows definitive diagnosis for conditions such as urethral diverticulum, leiomyoma, adenomyosis, endometriosis, and dermoid

• Uterine malignancy

- Endometrial cancer
 - Preoperative staging: deep myometrial invasion correlated with lymph node invasion [5, 6]
 - MRI shown to aid management for advanced and high grade cancer [7]
- Cervical carcinoma
 - Depth of stromal and parametrial invasion [8, 9]
 - MRI particularly aids management for
 - Tumors larger than 2 cm
 - Endocervical tumors [10]
 - Biopsy-proved adenocarcinoma (cervical versus endometrial origin)
 - Coexistent pelvic mass(es)
 - New diagnosis of cervical cancer during pregnancy
 - Prior radiation therapy [11–15]

• Adnexal mass

- Determine origin of mass
- Tissue characterization aids specific diagnosis (e.g., endometrioma, dermoid)
- MRI helps predict likelihood of malignancy to direct proper management and limit surgical intervention for benign disease [16, 17]
- For known ovarian cancer, CT typically used for staging; MRI if CT contraindicated
- MRI may yield definitive diagnosis for adnexal disease that is indeterminate on ultrasound, obviating need for follow-up imaging

• Abdominal pain in pregnancy

- Accurate evaluation for appendicitis (and other acute diseases) without ionizing radiation [18, 19]
- Increasing availability of MRI in acute setting

• Fetal anomalies

- Problem solving for indeterminate ultrasound
- Usefulness of MRI has increased with ultrafast sequences

Table 1.1. Indications for MRI of the female pelvis

Indication	Protocol	Notes
Pelvic pain	General	FS T1WI for endometriosis
Urethral diverticulum	Urethra	Contrast if known/visualized mass
Vaginal mass	Urethra	Contrast if known/visualized mass
Pelvic floor symptoms	Pelvic floor	Sagittal images with Valsalva
Uterine anomaly	Uterine anomaly	True coronal to uterine fundus
Adenomyosis	General	Bright myometrial foci on T2WI
Fibroids	General	Add contrast if pre-embolization
Fibroid versus adnexal mass	General	Vessels extending from uterus to mass suggest uterine origin
Endometrial cancer	Uterine malignancy	High resolution T2WI and T1WI + contrast oblique to endometrium for tumor invasion
Cervical cancer	Uterine malignancy	High resolution T2WI oblique to cervix for parametrial invasion
Adnexal mass characterization	General	FS T1WI for dermoid, endometrioma
Abdominal pain in pregnancy	Maternal abdominal pain	SS-ETSE (+ FS), and steady-state GE for appendix, monitor if possible
Fetal anomaly	Fetal	SS-ETSE oriented to region of interest, monitor if possible

FS = fat saturated; T1WI = T1-weighted images; T2WI = T2-weighted images; SS = single shot; ETSE = echo-train spin-echo; GE = gradient echo

Patient preparation for MRI

- Empty bladder
- Fasting 4 hours
- Optional
 - Antispasmodic (e.g., glucagon 1 mg)
 - Intra-vaginal gel [20]
- Supine position, or decubitus in late pregnancy
- Phased-array coil positioned over pelvis
- To reduce artifact, may utilize
 - Saturation band over anterior abdominal wall for non-fat-saturated sagittal
 - Supplemental anteroposterior frequency-encoding direction for axial images
- Intrauterine contraceptive devices are safely imaged [21]

Sequence protocols

- Many protocol options
- Appropriate choice depends on
 - Specific clinical question
 - Available equipment and expertise

- For known or suspected uterine disease/anomalies, T2-weighted sequences are obtained in an oblique plane oriented to uterus (Figure 1.1)
- Individual sequence parameters may vary based on manufacturer, etc.
- Sequences may include
 - Single-shot (SS) echo-train spin echo (ETSE)
 - For example, HASTE or SSFSE
 - Sensitive to fluid, resistant to motion and susceptibility
 - Large field of view
 - Localization, evaluation of coil position
 - Coronal: evaluation of renal anomalies/obstruction
 - Axial: prescribe true sagittal view of uterus
 - T2-weighted
 - Breathhold may be sufficient for benign disease
 - Non-breathhold (high-resolution) for uterine malignancy
 - With or without fat saturation
 - May be done as 3D ETSE
 - Best sequence for uterine zonal anatomy
 - T1-weighted

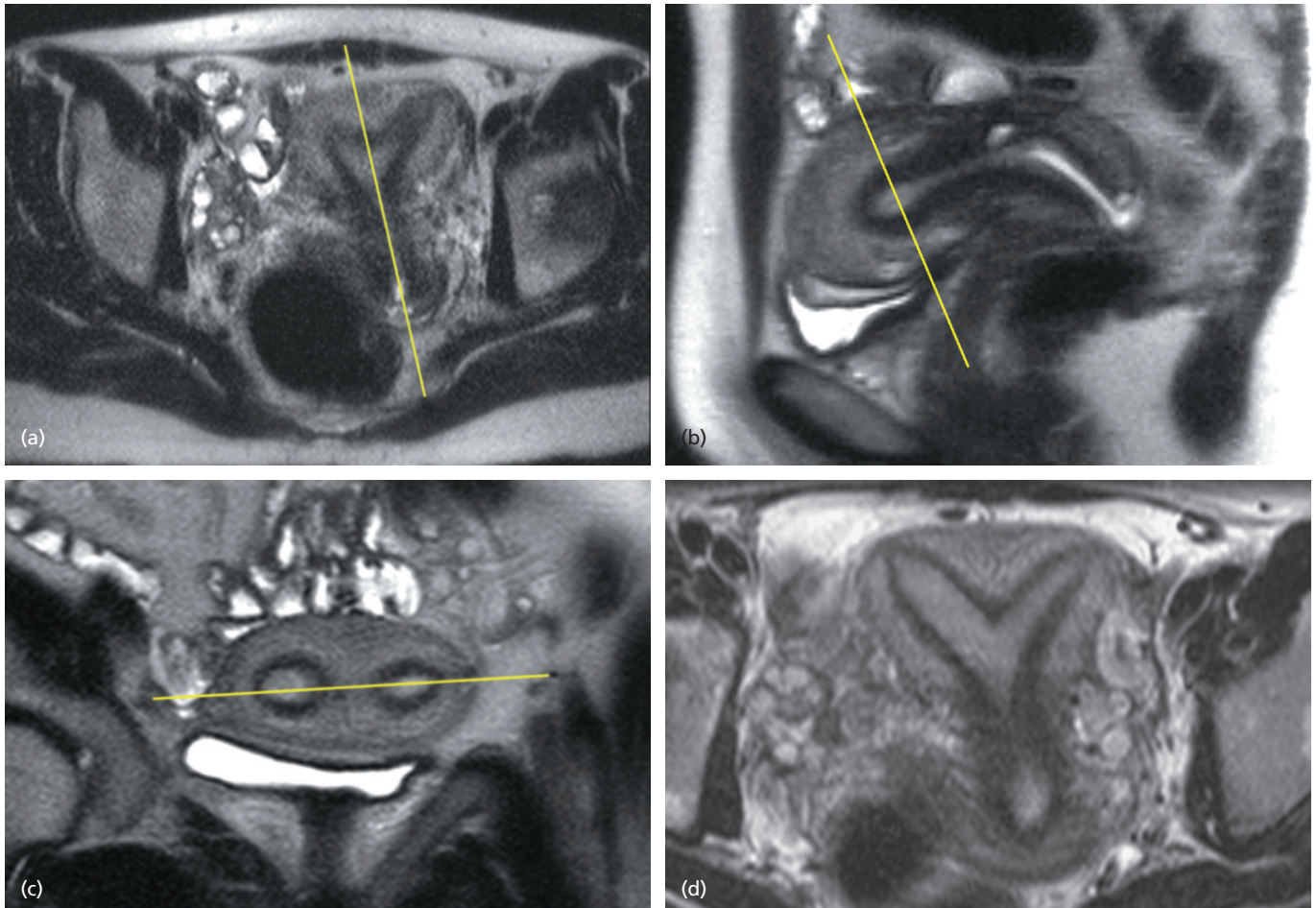


Figure 1.1. Imaging planes oriented to the uterus. Multiple T2-weighted images in a patient with septate uterus. Large field-of-view single-shot sequence **(a)** is obtained first and is used to plan an oblique sagittal T2-weighted sequence **(b)** obtained parallel to the endometrium (line, **a**). The oblique sagittal is used to plan an oblique axial **(c)** obtained perpendicular to the endometrium (line, **b**). The oblique axial may then be used to plan a true coronal of the uterus **(d)** obtained parallel to the endometrium (line, **c**). In the absence of 3D T2-weighted imaging, this process assures appropriate imaging planes regardless of angle/tilt of the uterus.

- Breathhold in- and out-of-phase dual echo
 - Differentiates fat- and blood-containing lesions
 - Sensitive to small foci of fat within adnexal mass
- Non-breathhold (high-resolution) for uterine cancer
- Chemically selective fat saturation for endometriosis
- T2/T1-weighted steady-state free precession gradient echo (GE)
 - For example, TruFISP or FIESTA
 - Rapid, resistant to motion
 - Differentiates vessels from bowel (e.g., appendix)
 - Useful for fetal and maternal imaging
- T1-weighted 3D GE pre- and post-contrast
 - Fat-suppressed GE, repeated for dynamic imaging
 - Provides enhancement information
 - May use MRA parameters (e.g., vascular malformation)
- Diffusion-weighted imaging (DWI) (optional)
 - B values of 0 and at least one other value up to 1000
 - Apparent diffusion coefficient (ADC) map created
 - DWI sequence and ADC map interpreted together
 - Aids detection of tumor, inflammation

- Additional functional techniques may have increasing role [7]
- Oblique planes oriented to the endometrium or cervix important for cancer [22]
- Protocol tailored to clinical question (Table 1.2, Table 1.3, Table 1.4, Table 1.5, Table 1.6, Table 1.7, Table 1.8)

Table 1.2. General female pelvis

Sequence	Plane	FOV (cm)	Slice thickness (mm)
SS-ETSE	Coronal	32	8
SS-ETSE	Axial	32	8
T2 ETSE	Sagittal	24	5
T2 ETSE	Axial	24	5
T1 GE in/out- of-phase	Axial	24	5
T1 GE FS	Axial	24	5
DWI (optional)	Axial	28	6
T1 3D GE FS (pre)	Axial or sagittal	24	3
<i>Contrast</i>			
T1 3D GE FS (post × 3)	Axial or sagittal	24	3
T1 GE FS (delayed)	Axial	24	5

SS = single shot; ETSE = echo-train spin-echo; GE = gradient echo; FS = fat saturated; DWI = diffusion-weighted imaging

Table 1.3. Urethra

Sequence	Plane	FOV (cm)	Slice thickness (mm)
SS-ETSE	Coronal	32	8
T2 ETSE	Coronal	16	4
T2 ETSE	Axial	16	4
T1 GE	Axial	16	4
T1 3D GE FS (pre)	Axial	24	3
<i>Contrast (if known or visualized lesion)</i>			
T1 GE FS (delayed)	Axial	24	3

SS = single shot; ETSE = echo-train spin-echo; GE = gradient echo; FS = fat saturated

Table 1.4. Pelvic floor

Sequence	Plane	FOV (cm)	Slice thickness (mm)
SS-ETSE	Coronal	32	8
SS-ETSE	Axial	32	8
SS-ETSE	Sagittal	32	5
SS-ETSE (Valsalva, repeat × 3)	Sagittal	32	5 (midline slice)

SS = single shot; ETSE = echo-train spin-echo

Table 1.5. Uterine anomaly

Sequence	Plane	FOV (cm)	Slice thickness (mm)
SS-ETSE	Coronal	32	8
SS-ETSE	Axial	32	8
T2 ETSE	Sagittal (to uterus)	24	5
T2 ETSE	Axial (to uterus)	24	5
T2 ETSE	Coronal (to uterus)	24	5
T1 GE in/out-of-phase	Coronal (to uterus)	24	5
T1 GE FS	Axial	24	5

SS = single shot; ETSE = echo-train spin-echo; GE = gradient echo; FS = fat saturated

Table 1.6. Uterine malignancy

Sequence	Plane	FOV (cm)	Slice thickness (mm)
SS-ETSE	Coronal	32	8
SS-ETSE	Axial	32	8
T2 ETSE	Sagittal	24	5
T2 ETSE	Axial	24	5
T1 GE in/out-of-phase	Axial	24	5
T1 GE FS	Axial	24	5
DWI (optional)	Axial	28	6
T1 3D GE FS (pre)	Axial or sagittal	24	3
<i>Contrast</i>			
T1 3D GE FS (post × 3)	Axial or sagittal	24	3
T1 GE FS (delayed)	Axial	24	5

SS = single shot; ETSE = echo-train spin-echo; GE = gradient echo; FS = fat saturated

Table 1.7. Maternal abdominal pain

Sequence	Plane	FOV (cm)	Slice thickness (mm)
SS-ETSE	Coronal	32–40	8
SS-ETSE	Axial	32	5
SS-ETSE FS	Axial	32	5
Steady-state GE	Coronal	32	5
Steady-state GE	Axial	32	5
T1 GE in/out-of-phase	Axial	32	5

SS = single shot; ETSE = echo-train spin-echo; GE = gradient echo; FS = fat saturated

Table 1.8. Fetal

Sequence	Plane	FOV (cm)	Slice thickness (mm)
SS-ETSE	Coronal	40	8
SS-ETSE	Axial	40	8
SS-ETSE	Sagittal	40	8
SS-ETSE (repeat as needed)	Directed	24–32	4–6
Steady-state GE (optional)	Directed	24–32	4–6
T1 GE in/out-of-phase (optional)	Directed	24–32	4–6

SS = single shot; ETSE = echo-train spin-echo; GE = gradient echo; FS = fat saturated

Image optimization at 3T

- Potential advantages
 - Increase in signal-to-noise ratio (SNR), or
 - Similar SNR at a faster speed
- Challenges
 - Signal shading magnified by dielectric effects
 - Increased specific absorption rates (SARs)
 - Changes in optimal TR and TE
 - Increased signal inhomogeneities
 - Greater shimming challenge for extrinsic magnetic field
 - Intrinsic field distortion due to increased susceptibility/chemical shift
- Solutions [23–28]
 - Dielectric effect: dielectric pad (= radiofrequency cushion) placed between patient and surface coil
 - Susceptibility: use shorter TE/higher receiver bandwidth, higher spatial resolution
 - 3D GE and ETSE sequences may benefit from higher field strength
 - Consider individual patient
 - Pregnant patients less suitable for 3T due to standing wave effects from amniotic fluid and safety concerns [26]
 - Non-pregnant patients may be imaged safely and effectively at 3T using optimized parameters [28]

Image interpretation

- Large volume data acquisition
- May be useful to employ a systematic checklist (Table 1.9)
- Several gynecological conditions have MRI features that allow definitive diagnosis

Table 1.9. Diagnostic checklist for female pelvis MRI

Structure	MRI features evaluated
Gynecological	
Uterine corpus	Size and position Presence of myometrial mass Endometrium thickness Junctional zone thickness
Cervix	Presence of cystic mass Presence of solid tumor Size of lesion Parametrial involvement
Vagina	Presence of cystic mass Presence of wall thickening/solid tumor
Adnexa	Ovarian size Presence of ovarian mass Cystic or solid Fat containing Blood containing Enhancement features Unilateral or bilateral Paraovarian cystic or solid mass
Non-gynecological	
Bladder	Presence of solid mass Presence of cystocele
Urethra	Presence of diverticulum Size and configuration Solid/enhancing components Presence of hypermobility
Bowel	Caliber Presence of rectocele
Musculoskeletal	Bone marrow signal Degenerative changes Traumatic injury
Lymphatic	Enlarged lymph nodes

References

- Lee, J.H., Dubinsky, T., Andreotti, R.F., et al. ACR Appropriateness Criteria(R) pretreatment evaluation and follow-up of endometrial cancer of the uterus. *Ultrasound Quarterly* 2011; 27(2):139–45.
- Siegel, C.L., Andreotti, R.F., Cardenas, H.R., et al. ACR Appropriateness Criteria(R) pretreatment planning of invasive cancer of the cervix. *Journal of the American College of Radiology* 2012; 9(6):395–402.
- Harris, R.D., Javitt, M.C., Glanc, P., et al. ACR Appropriateness Criteria(R) clinically suspected adnexal mass. *Ultrasound Quarterly* 2013; 29(1):79–86.
- Andreotti, R.F., Lee, S.I., Dejesus Allison, S.O., et al. ACR Appropriateness Criteria(R) acute pelvic pain in the reproductive age group. *Ultrasound Quarterly* 2011; 27(3):205–10.
- Kinkel, K., Kaji, Y., Yu, K.K., et al. Radiologic staging in patients with endometrial cancer: a meta-analysis. *Radiology* 1999; 212(3):711–18.
- Wakefield, J.C., Downey, K., Kyriazi, S., deSouza, N.M. New MR techniques in gynecologic cancer. *AJR. American Journal of Roentgenology* 2013; 200(2):249–60
- Frei, K.A., Kinkel, K., Bonél, H.M., et al. Prediction of deep myometrial invasion in patients with endometrial cancer: clinical utility of contrast-enhanced MR imaging – a meta-analysis and Bayesian analysis. *Radiology* 2000; 216(2):444–9.
- Sironi, S., De Cobelli, F., Scarfone, G., et al. Carcinoma of the cervix: value of plain and gadolinium-enhanced MR imaging in assessing degree of invasiveness. *Radiology* 1993; 188(3):780–97.
- Subak, L.L., Hricak, H., Powell, C.B., Azizi, L., Stern, J.L. Cervical carcinoma: computed tomography and magnetic resonance imaging for preoperative staging. *Obstetrics and Gynecology* 1995; 86(1):43–50.
- Hricak, H., Powell, C.B., Yu, K.K., et al. Invasive cervical carcinoma: role of MR imaging in pretreatment work-up – cost minimization and diagnostic efficacy analysis. *Radiology* 1996; 198(2):403–9.
- Flueckiger, F., Ebner, F., Poschauko, H., et al. Cervical cancer: serial MR imaging before and after primary radiation therapy – a 2-year follow-up study. *Radiology* 1992; 184(1):89–93.
- Hricak, H., Swift, P.S., Campos, Z., et al. Irradiation of the cervix uteri: value of unenhanced and contrast-enhanced MR imaging. *Radiology* 1993; 189(2):381–8.
- Weber, T.M., Sostman, H.D., Spritzer, C.E., et al. Cervical carcinoma: determination of recurrent tumor extent versus radiation changes with MR imaging. *Radiology* 1995; 194(1):135–9.
- Yamashita, Y., Harada, M., Torashima, M., et al. Dynamic MR imaging of recurrent postoperative cervical cancer. *Journal of Magnetic Resonance Imaging* 1996; 6(1):167–71.
- Hertel, H., Köhler, C., Grund, D., et al. Radical vaginal trachelectomy (RVT) combined with laparoscopic pelvic lymphadenectomy: prospective multicenter study of 100 patients with early cervical cancer. *Gynecologic Oncology* 2006; 103(2): 506–11.

16. Hricak, H., Chen, M., Coakley, F.V., et al. Complex adnexal masses: detection and characterization with MR imaging – multivariate analysis. *Radiology* 2000; 214(1):39–46.
17. Sohaib, S.A., Sahdev, A., Van Trappen, P., Jacobs, I.J., Reznick, R.H. Characterization of adnexal mass lesions on MR imaging. *AJR. American Journal of Roentgenology* 2003; 180(5):1297–304.
18. Birchard, K.R., Brown, M.A., Hyslop, W.B., Firat, Z., Semelka, R.C. MRI of acute abdominal and pelvic pain in pregnant patients. *AJR. American Journal of Roentgenology* 2005; 184(2):452–8.
19. Oto, A., Ernst, R.D., Shah, R., et al. Right-lower-quadrant pain and suspected appendicitis in pregnant women: evaluation with MR imaging – initial experience. *Radiology* 2005; 234(2):445–51.
20. Brown, M.A., Mattrey, R.F., Stamato, S., Sirlin, C.B. MRI of the female pelvis using vaginal gel. *AJR. American Journal of Roentgenology* 2005; 185(5):1221–7.
21. Pasquale, S.A., Russer, T.J., Foldes, R., Mezrich, R.S. Lack of interaction between magnetic resonance imaging and the copper-T380A IUD. *Contraception* 1997; 55(3): 169–73.
22. Shiraiwa, M., Joja, I., Asakawa, T., et al. Cervical carcinoma: efficacy of thin-section oblique axial T2-weighted images for evaluating parametrial invasion. *Abdominal Imaging* 1999; 24(5): 514–19.
23. Kataoka, M., Kido, A., Koyama, T., et al. MRI of the female pelvis at 3T compared to 1.5T: evaluation on high-resolution T2-weighted and HASTE images. *Journal of Magnetic Resonance Imaging* 2007; 25(3): 527–34.
24. Martin, D.R., Friel, H.T., Danrad, R., De Becker, J., Hussain, S.M. Approach to abdominal imaging at 1.5 Tesla and optimization at 3 Tesla. *Magnetic Resonance Imaging Clinics of North America* 2005; 13(2):241–54.
25. Hussain, S.M., van den Bos, I.C., Oliveto, J.M., Martin, D.R. MR imaging of the female pelvis at 3T. *Magnetic Resonance Imaging Clinics of North America* 2006; 14(4):537–44.
26. Merkle, E.M., Dale, B.M. Abdominal MRI at 3.0 T: the basics revisited. *AJR. American Journal of Roentgenology* 2006; 186(6):1524–32.
27. Cornfeld, D., Weinreb, J. Simple changes to 1.5-T MRI abdomen and pelvis protocols to optimize results at 3T. *AJR. American Journal of Roentgenology* 2008; 190(2): W140–50.
28. Morakkabati-Spitz, N., Schild, H.H., Kuhl, C.K., et al. Female pelvis: MR imaging at 3.0 T with sensitivity encoding and flip-angle sweep technique. *Radiology* 2006; 241(2): 538–45.

Chapter 2

Imaging the vagina and urethra

Shannon St. Clair, Randy Fanous, Mohamed El-Azzazi, Richard C. Semelka, & Michele A. Brown

Vagina

Normal anatomy

Key facts

- Fibromuscular tube between bladder and rectum, 7–9cm long (Figure 2.1) Embryological origin [1]
 - Upper one-third = Müllerian duct
 - Lower two-thirds = urogenital sinus
- Layers [2]
 - Inner = mucosa
 - Middle = submucosa and muscularis
 - Outer = adventitia, containing vaginal venous plexus
- Fornices: anterior, posterior, lateral
 - Portion of vagina that surrounds the cervix
 - Best visualized on sagittal and transverse images

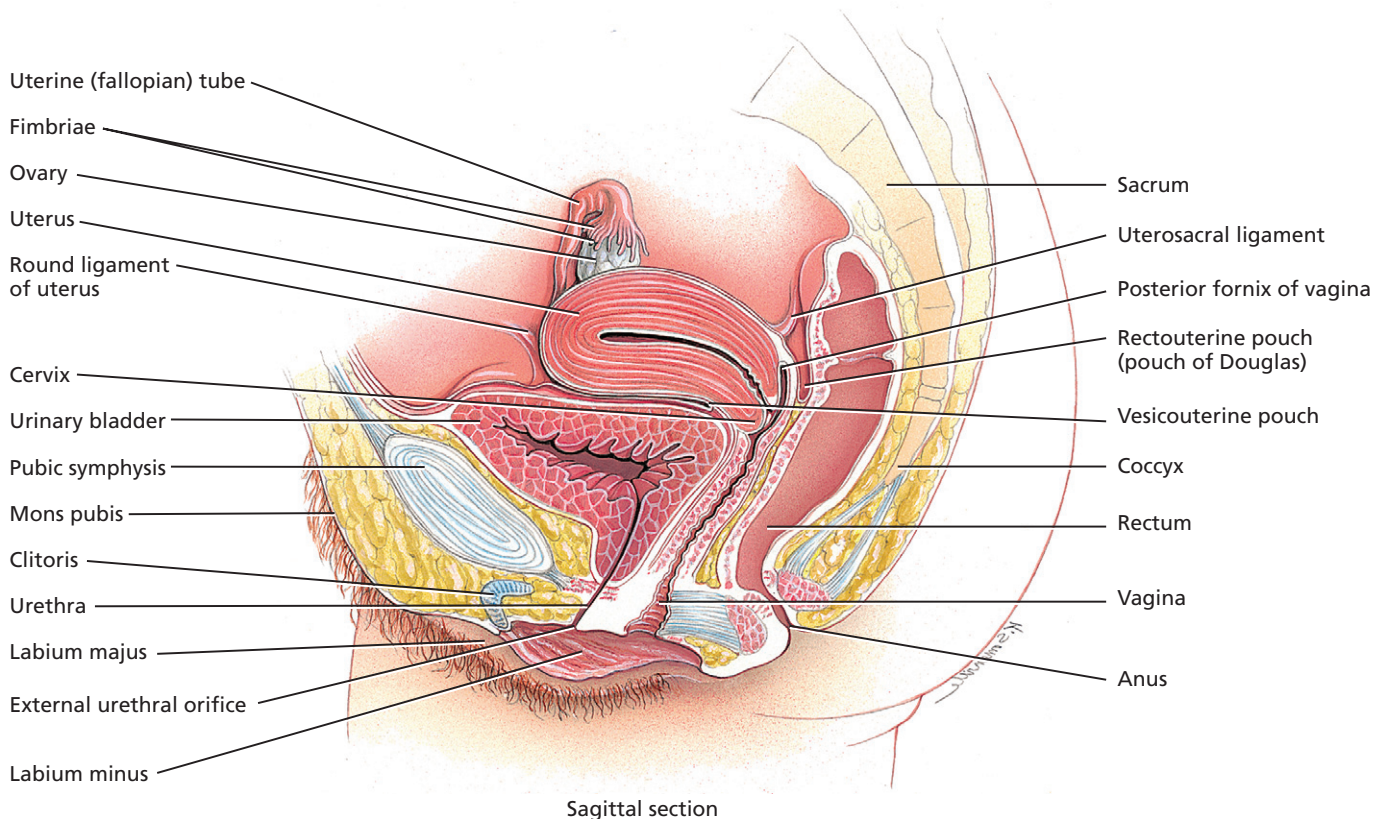


Figure 2.1. Normal female pelvic anatomy in the sagittal plane. (Source: Tortora & Derrickson (Eds), Principles of Anatomy and Physiology, 13th edn. Hoboken, NJ: Wiley, 2012.)

- For descriptive purposes, vagina may be divided into thirds
 - Upper third = level of the lateral fornices
 - Middle third = level of the bladder base
 - Lower third = level of the urethra

MRI features

- T1WI – low signal intensity
- T2WI
 - Stratified: outer high signal intensity, middle low signal intensity, inner high signal intensity
 - Thickness correlates with estrogen level; most prominent during late proliferative and early secretory phases of menstrual cycle (Figure 2.2)
 - Loss of normal stratification
 - Pregnant = outer and middle intermediate to high signal intensity, inner high signal intensity
 - Premenarchal/ postmenopausal = outer and middle low signal intensity, markedly thin inner high signal intensity
- T1WI + contrast – avid early enhancement of outer and middle layers only

Vaginal agenesis/atresia

Key facts

- Rare Müllerian duct anomaly ranging from complete to partial agenesis
 - Incidence of all Müllerian duct anomalies in women is 1–15%
 - 1 in 4000–5000 women have vaginal agenesis [3, 4]
- Typically normal ovaries and external genitalia, however associated abnormalities of the uterus, cervix, upper urinary tract, and skeleton may occur
- Presentation depends on presence of functioning endometrium
 - If no functioning endometrium = primary amenorrhea
 - If functioning endometrium present = pain and mass effect at the age of menarche secondary to hematometra (Figure 2.3)
- Untreated patients with functional endometrium may develop endometriosis
- Surgical management depends on presence of functioning endometrium and cervix
 - Complete agenesis + small rudimentary uterine bulb with no functioning endometrium = vaginoplasty

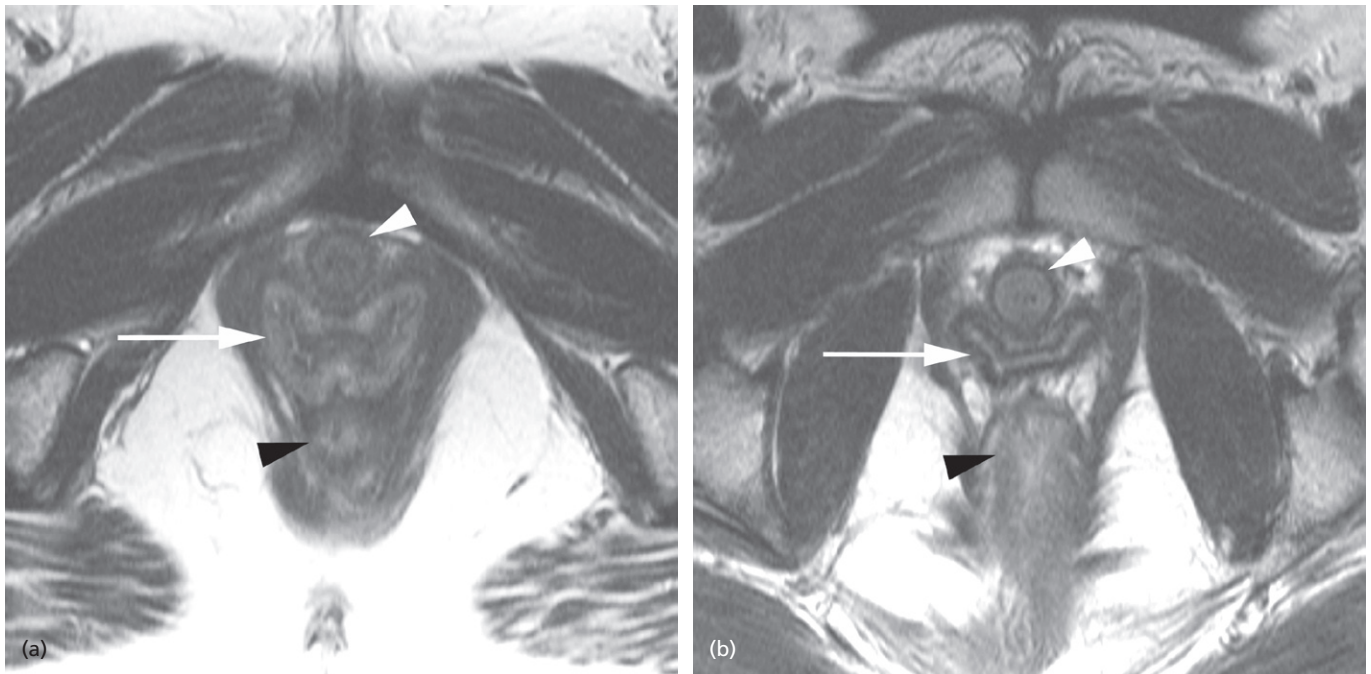


Figure 2.2. Normal vagina in two patients. Axial T2-weighted image in two patients (**a, b**) show variable thickness in the vagina depending on estrogen levels. Note vagina (arrow), urethra (white arrowhead), and rectum (black arrowhead).

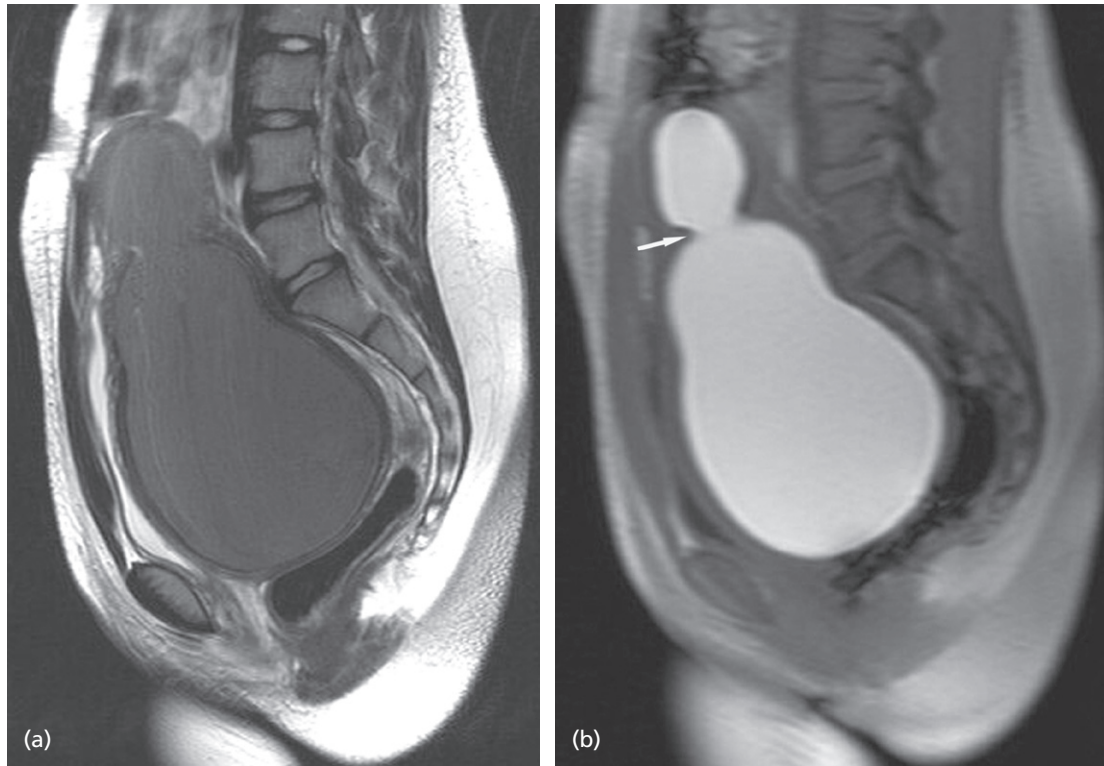


Figure 2.3. Vaginal atresia with hematometocolpos. Sagittal T2-weighted **(a)** and T1-weighted **(b)** images show the upper vagina and uterus are dilated and blood filled. Narrowing of the blood-filled structures is noted at the level of the cervix (arrow, **b**). Note absence of the distal vagina inferior to the blood-filled mass, best appreciated on T2WI. This finding helps distinguish from imperforate hymen or obstructing vaginal septum.

- Complete agenesis + small rudimentary uterine bulb with functioning endometrium = vaginoplasty + hysterectomy
- Complete agenesis + uterus with endometrium but no cervix = vaginoplasty + hysterectomy
- Partial agenesis + normal uterus and cervix = creation of an external vaginal os (i.e., fertility potential restored)
- Mayer–Rokitansky–Küster–Hauser syndrome [5]
 - Vaginal and uterine agenesis, with normal tubes and ovaries and variable urinary tract anomalies (Figure 2.4)
 - 1 in 5000 female births
 - Most patients have a normal karyotype
 - Uterine and/or vaginal rudiments may be present; important for surgical planning

MRI features

- Thin-section transverse T2WI best
- Sagittal to delineate vaginal length if partial agenesis; important for surgical planning
- Demonstrates presence or absence of the uterus, cervix, and kidneys
- T1WI used to identify blood products of functioning endometrial tissue

Vaginal duplication and septa

Key facts

- Duplication typically occurs in the setting of uterus didelphys
 - Associated with renal agenesis
 - Longitudinal septum may result in dyspareunia

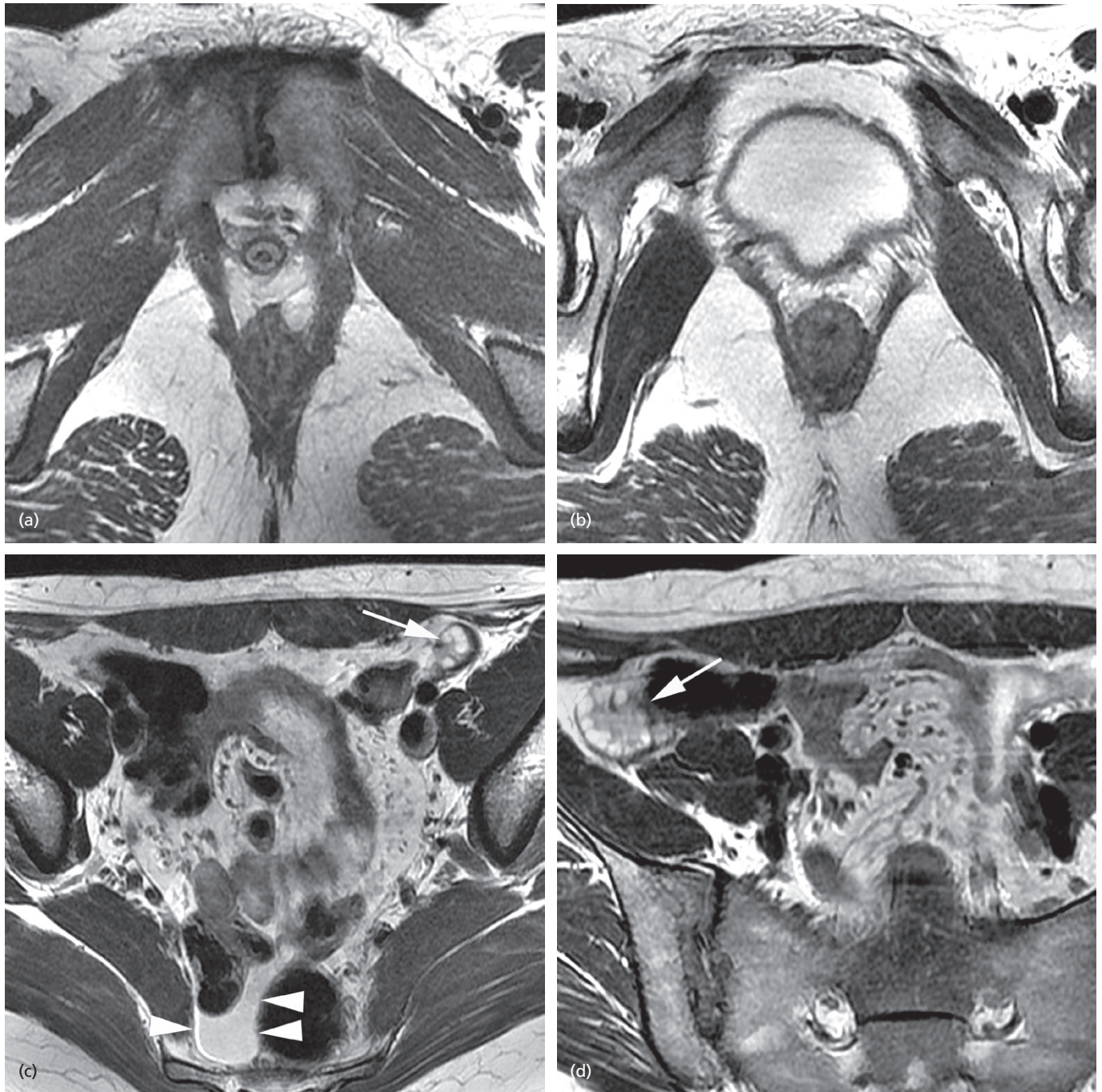


Figure 2.4. Mayer–Rokitansky–Küster–Hauser syndrome. Axial T2-weighted images (a–d) show vaginal and uterine agenesis with only fat seen between the urethra and rectum. Both ovaries (arrows, c, d) are superiorly positioned but otherwise normal; note physiologic fluid in the pelvis (arrowheads, c).

- Transverse septum may occur without Müllerian anomaly [6, 7]
 - Failure of fusion of the down-growing Müllerian duct with the up-growing urogenital sinus
 - Results in obstruction
 - Presents at puberty with amenorrhea and cyclical abdominal pain
- Thin-section T2-weighted transverse images are optimal
- Untreated patients may develop endometriosis
- Surgical management
 - Vaginal reconstruction with resection of longitudinal/transverse septa
 - Vaginoplasty and hysterectomy, if associated cervical agenesis [4, 6, 7]

MRI features

- Hematocolpos if obstruction present – variable signal intensity on T1WI and T2WI (Figure 2.5)
- Vaginal and/or uterine duplication if associated Müllerian anomaly

Abnormalities of gonadal differentiation

Key facts

- Gonadal dysgenesis
 - Pure-type
 - Bilateral streak gonads – i.e., fibrous lesions, without germ cells [8]
 - Majority have Turner's syndrome
 - Mixed-type
 - Mosaic karyotypes (XO/XY and XO/XYY)
 - One testis, one streak gonad
 - Y chromosome-containing gonads at increased risk for malignant transformation; should be removed
- True hermaphrodites
 - Ovarian and testicular tissue, together as ovotestis or separate discrete gonads [8]
 - 80% XX karyotype, remaining either XY or mosaic [9]
 - Sex assignment typically determined by external genitalia
 - Ovotestes, testes, or ovaries typically intra-abdominal and at increased risk of malignancy

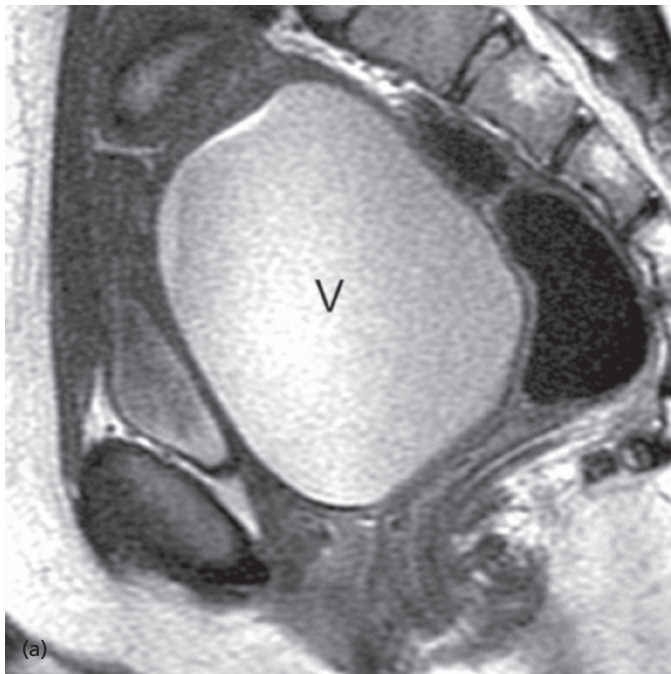


Figure 2.5. Transverse vaginal septum and hematocolpos. Sagittal T2-weighted image **(a)** in a young woman with pelvic pain shows a distended vaginal canal (V) that is filled with complex fluid. Axial T2-weighted image **(b)** distal to the septum shows a normal vaginal canal (arrow, **b**). Demonstration of a normal distal vagina helps distinguish this entity from imperforate hymen or vaginal atresia on MR imaging.

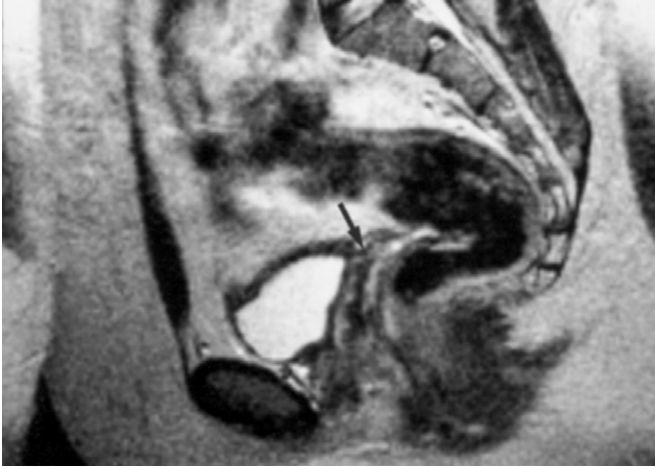


Figure 2.6. Testicular feminization. Sagittal T2-weighted image shows absent uterus and blind-ending vagina (arrow).

- Pseudohermaphrodites
 - Normal genotype, but ambiguous genitalia
 - Male pseudohermaphrodites:
 - Testes with ambiguous genitalia [8]
 - Most commonly testicular feminization (Figure 2.6)
 - X-linked recessive disorder of absent cytoplasmic testosterone receptors
 - Phenotypically female, blind-ended vagina with no uterus or fallopian tubes
 - T2-weighted MR imaging helpful in preoperative location of testes, which are removed due to risk of malignancy
 - Female pseudohermaphrodites:
 - 46 XX karyotype, normal ovaries, virilized external genitalia secondary to *in utero* androgen exposure [8]
 - Most commonly 21-hydroxylase deficiency, which is one form of congenital adrenal hyperplasia
 - More rare causes include androgen-producing tumors or maternal ingestion of androgen-containing drugs during the first trimester
 - With surgical and/or hormonal treatment, these females can have normal fertility and near-normal female phenotype

MRI features

Streak gonads

- T2WI – small and low signal intensity



Figure 2.7. Asymptomatic Bartholin cyst. Sagittal T2-weighted image shows a cystic lesion at the posterolateral distal vagina (arrow).

Bartholin cyst

Key facts

- Mucus secreting glands drain into posterolateral vaginal vestibule [10]
- Chronic inflammation or trauma leads to mucous retention and cyst formation
- Typically asymptomatic, unless superinfection (e.g., *Neisseria gonorrhoeae*)
- Treatment options: antibiotic therapy, aspiration, incision and drainage, laser vaporization, and marsupialization

MRI features

- Location – posterolateral wall of the lower third of the vagina [10]
- T1WI – intermediate to high signal intensity, depending on the protein content (Figure 2.7)
- T2WI – high signal intensity
- T1WI + contrast – rim enhancement, suggests infection

Gartner duct cyst

Key facts

- Mesonephric or wolffian duct remnant
- Most common benign vulvovaginal lesion in children
- Incidentally identified in 1–2% of female pelvic MRI examinations [11]

- Typically asymptomatic, however larger lesions may cause dyspareunia or difficult vaginal delivery
 - Associated with genitourinary abnormalities, e.g., ipsilateral renal agenesis (Herlyn–Werner–Wunderlich syndrome) [12]

MRI features

- Location – anterolateral wall of the lower upper third of the vagina
- T1WI – low signal intensity (most) versus intermediate to high signal intensity (depending on amount proteinaceous or hemorrhagic contents) (Figure 2.8)

- T2WI – high signal intensity
- T1WI + contrast – typically no rim enhancement

Cavernous hemangioma

Key facts

- Rare benign lesion of the vulva or vagina
- Most common in infants, tends to stabilize or regress during childhood
- Typically asymptomatic, however may cause bleeding, ulceration or hemorrhage during vaginal delivery [13]

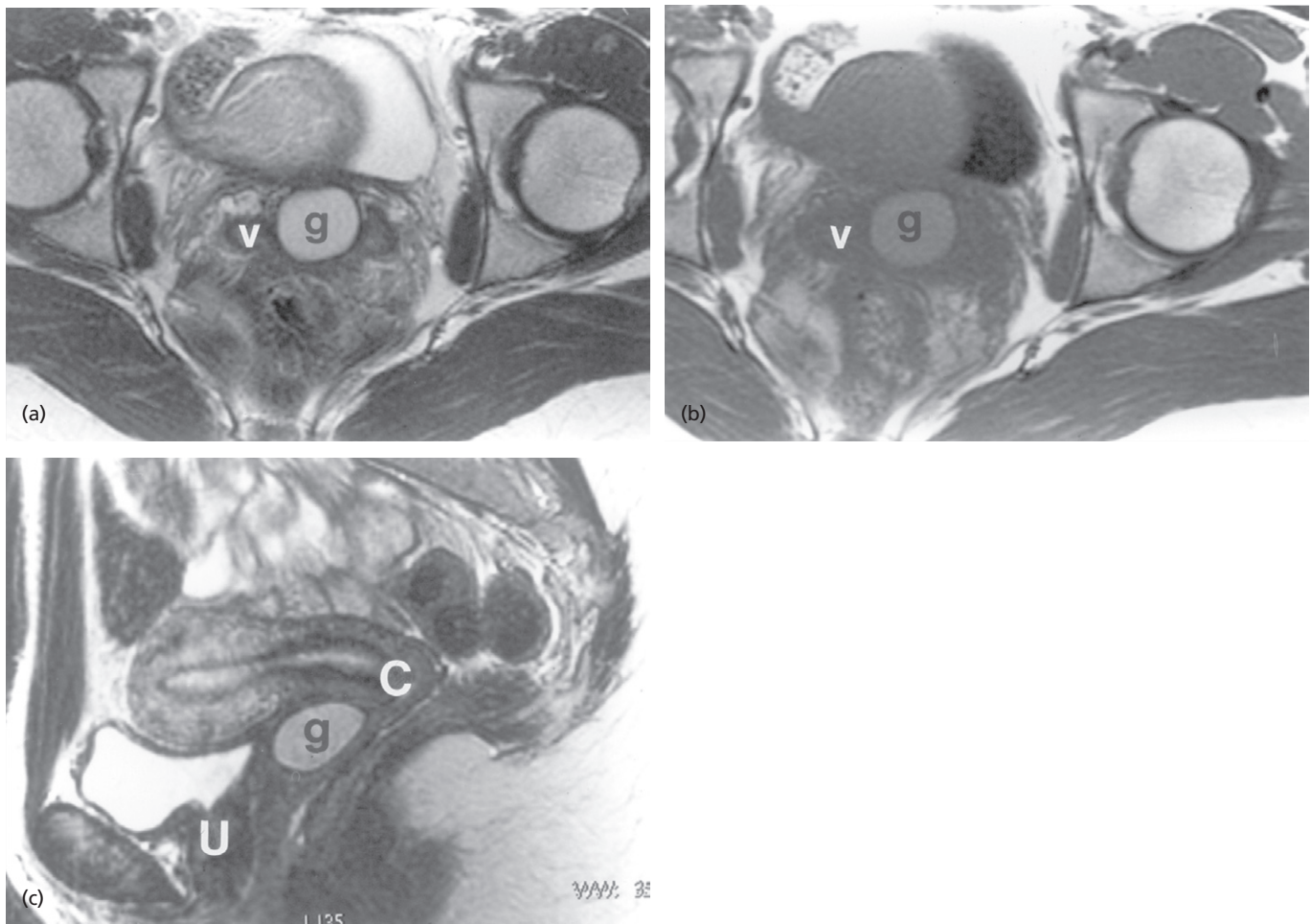


Figure 2.8. Gartner duct cyst. Axial T2-weighted (a), T1-weighted (b), and sagittal T2-weighted (c) images in a patient with an asymptomatic palpable paracervical mass. There is a well-circumscribed mass with high-signal-intensity (g, a–c), centered within the left side of the proximal vagina (v, a, b). The high signal on T1WI reflects intracystic protein. Sagittal T2-weighted image (c) reveals that the mass is located above the urethra (U, c) and below the cervix (C, c) within the proximal vagina. The normal zonal anatomy of the uterus is present.

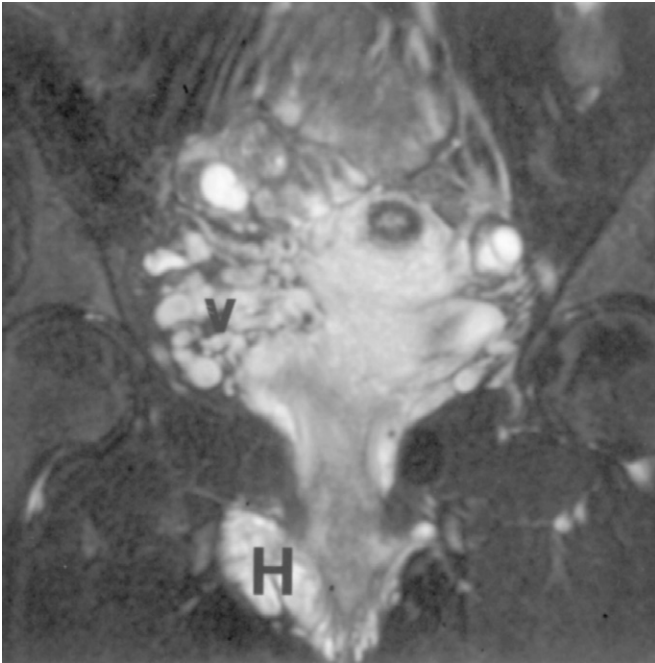


Figure 2.9. Vulvar cavernous hemangioma. Coronal fat-suppressed T2-weighted image in a patient with a spongy palpable vulvar mass shows a lobular hemangioma (H) in the region of the right vulva. Note asymmetric prominence of ipsilateral pelvic veins (v) due to the malformation.

MRI features

- T2WI – high signal intensity in the serpentine vascular lakes (Figure 2.9)
- T1WI + contrast – heterogeneous enhancement

Vaginal cancer

Key facts

- Most vaginal cancers are metastatic (usually from cervix or vulva) [14]
- Primary vaginal cancers account for less than 3% of all gynecological cancers
- Up to 95% of primary vaginal malignancies are of squamous cell histology, usually well differentiated [15]
- Typically affects older patients, peak incidence of 60–70 years
- Infection with human papillomavirus is a risk factor [14]
- FIGO classification schemes are most commonly used for staging (Table 2.1) [16, 17]
- Overall 5 year survival rate for all stages is 40% (Stage I 68%; Stage IV 20%) [15]

Table 2.1. FIGO staging for carcinoma of the vagina [16]

Stage	Description
I	Tumor limited to vaginal wall
II	Involves subvaginal tissue but has not extended to pelvic wall
III	Extends to pelvic wall
IV	Extends beyond true pelvis or involves mucosa of bladder or rectum
IVa	Invades bladder and/or rectal mucosa and/or direct extension beyond true pelvis
IVb	Spread to distant organs

Source: FIGO Committee on Gynecologic Oncology [16].

- Tumors in the upper third of the vagina spread to iliac nodes, whereas those in the lower two-thirds spread to inguinal nodes
- Melanoma is the second most common vaginal primary cancer
- Primary vaginal clear cell adenocarcinoma is associated with *in utero* diethylstilbestrol (DES) exposure
- Other rare primary vaginal malignancies include:
 - Leiomyosarcomas – poor prognosis
 - Lymphoma
 - Endodermal sinus tumors – infants, poor prognosis
 - Embryonal rhabdomyosarcoma (sarcoma botryoides) – children

MRI features

Squamous cell carcinoma

- Location – typically arise from the posterior wall of the upper third of the vagina (Figure 2.10)
- T1WI – intermediate signal intensity, often occult
- T2WI – moderate to high signal intensity
- T1WI + contrast – variable

Melanoma

- T1WI – may be high signal intensity (i.e. secondary to either intratumoral hemorrhage or from T1-shortening effects of paramagnetic metals such as iron that are associated with melanin [18])

Clear cell adenocarcinoma

- Location – typically arise from the anterior wall of the upper third of the vagina (Figure 2.11)

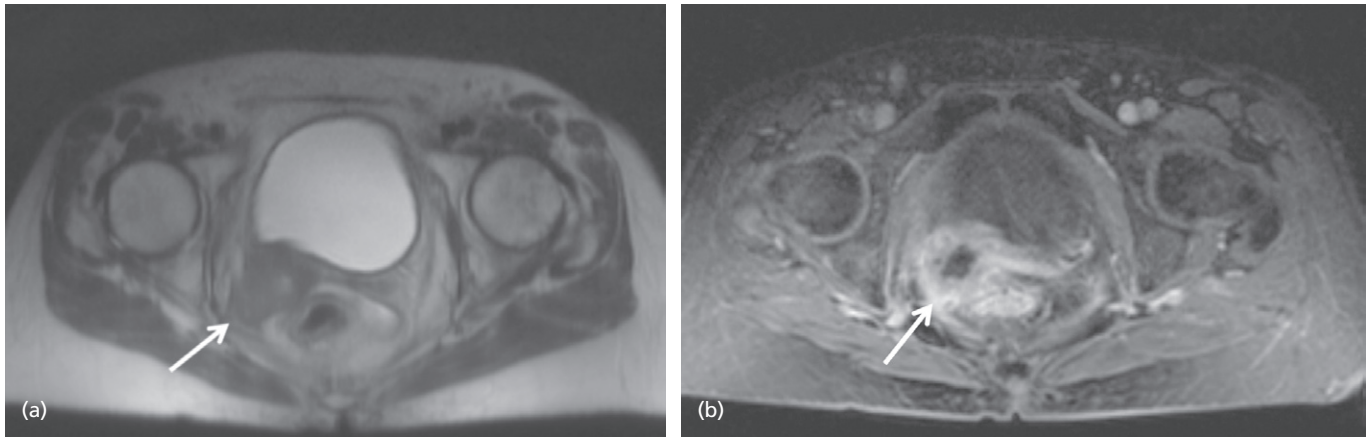


Figure 2.10. Vaginal carcinoma. Axial T2-weighted (a) and post-gadolinium fat-suppressed T1-weighted (b) images show an irregular, enhancing, partially necrotic vaginal mass (arrow).

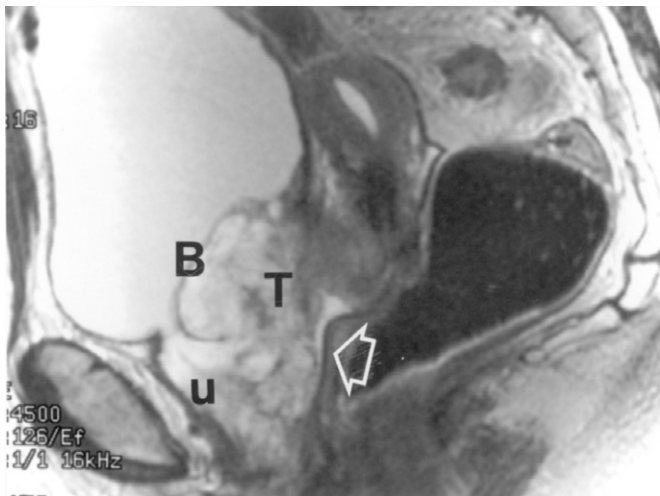


Figure 2.11. Clear cell adenocarcinoma of the vagina. Sagittal T2-weighted image shows a large heterogeneous intermediate to high-signal-intensity mass (T) in the anterior wall of the proximal vagina with gross invasion of the posterior bladder wall (B) and the posterior urethra (u). The posterior vaginal wall is preserved (white arrow).

Differentiating post-therapeutic changes from residual/recurrent disease:

- T2WI – tumor is typically high signal intensity on T2WI with irregular contours, whereas granulation tissue is typically low signal intensity on T2WI with smooth contours; however post-radiation changes within the first

year may also demonstrate high signal intensity and mimic tumor recurrence [19]

- T1WI + contrast – tumor typically demonstrates intense heterogeneous enhancement, whereas granulation tissue typically demonstrates more delayed homogeneous enhancement

Vaginal metastases

Key facts

- Secondary vaginal malignancies make up 80% of all vaginal cancers [14]
- Local spread from cervical or vulvar cancers comprise the majority of cases
- MRI technique should include T2-weighted and T1-weighted fat-suppressed post-gadolinium images in axial and sagittal planes

MRI features

- T1WI, T2WI, T1WI + contrast – signal intensity typically indistinguishable from that of primary vaginal squamous cell carcinoma, however may see primary tumor (Figure 2.12)

Vulvar carcinoma

Key facts

- Typically of squamous cell origin
- Typically older patients with pruritus (pain, bleeding, and palpable mass may also occur)

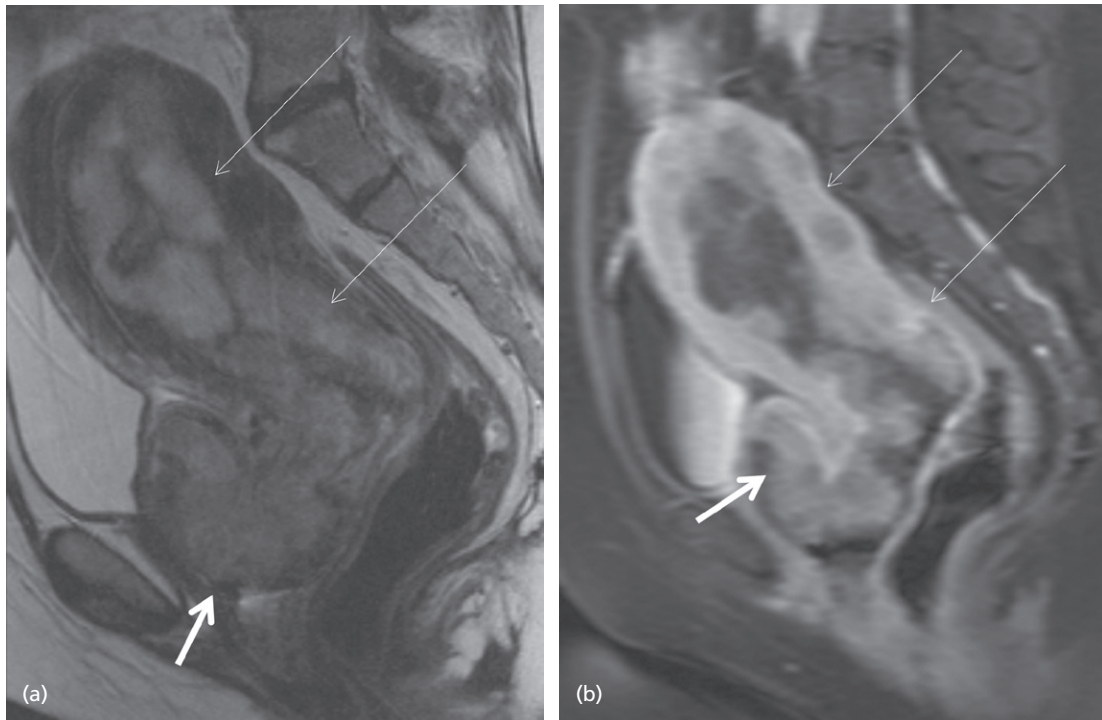


Figure 2.12. Vaginal invasion of cervical carcinoma. Sagittal T2-weighted **(a)** and post-gadolinium fat-suppressed T1-weighted **(b)** images show cervical carcinoma with extensive uterine (long arrows, **a**) and vaginal invasion (short arrow).

- FIGO system most commonly used for staging (Table 2.2) [20,21]
- Management options includes local resection with inguinal lymph node dissection, sentinel node mapping and biopsy, and/or adjuvant radiation therapy [14]
- Other rare primary vulvar malignancies include [14]:
 - Basal cell carcinoma
 - Adenocarcinoma – most arise in Bartholin’s gland
 - Melanoma
 - Sarcoma

MRI features

- T2WI – irregular mass, low to Intermediate signal intensity (Figure 2.13)
- T2WI – intermediate signal intensity
- T1WI + contrast – delayed enhancement

Radiation change

Key facts

- Imaging appearance of radiation change varies depending on the time interval between therapy and imaging

- Acute radiation changes (less than 1 year post-treatment) reflect histologic changes of interstitial edema and capillary leakage
- Chronic changes (more than 1 year post-treatment) reflects histologic changes of fibrosis with diminished interstitial fluid and vascularity; mural necrosis with secondary fistula formation may also occur [19, 22]

MRI features

Acute:

- T2WI – mural thickening with high signal intensity (Figure 2.14)
- T1WI + contrast – avid enhancement

Chronic:

- T2WI – mural thinning with low signal intensity
- T1WI + contrast – diminished enhancement
- Fistulas may appear as high-signal-intensity tract with enhancing rind

Table 2.2. FIGO staging for carcinoma of the vulva [21]

Stage	Description
I	Tumor confined to vulva
IA	≤2 cm, confined to vulva/perineum, stromal invasion ≤1.0 mm, no nodal metastasis
IB	>2 cm or stromal invasion >1.0 mm ^b , confined to vulva/perineum, negative nodes
II	Extension to adjacent perineal structures (1/3 lower urethra, 1/3 lower vagina, anus) with negative nodes
III	+/- extension to adjacent perineal structures (1/3 lower urethra, 1/3 lower vagina, anus) with positive inguino-femoral nodes
IIIA	(i) With 1 lymph node metastasis (≥5 mm)
	(ii) 1–2 lymph node metastasis(es) (<5 mm)
IIIB	(i) With 2 or more lymph node metastases (≥5 mm)
	(ii) 3 or more lymph node metastases (<5 mm)
IIIC	Positive nodes with extracapsular spread
IV	Invades other regional (2/3 upper urethra, 2/3 upper vagina), or distant structures
IVA	(i) upper urethral and/or vaginal, bladder, or rectal mucosa, or fixed to pelvic bone
	(ii) fixed or ulcerated inguino-femoral lymph nodes
IVB	Any distant metastasis including pelvic lymph nodes

Source: Pecorelli S [21].

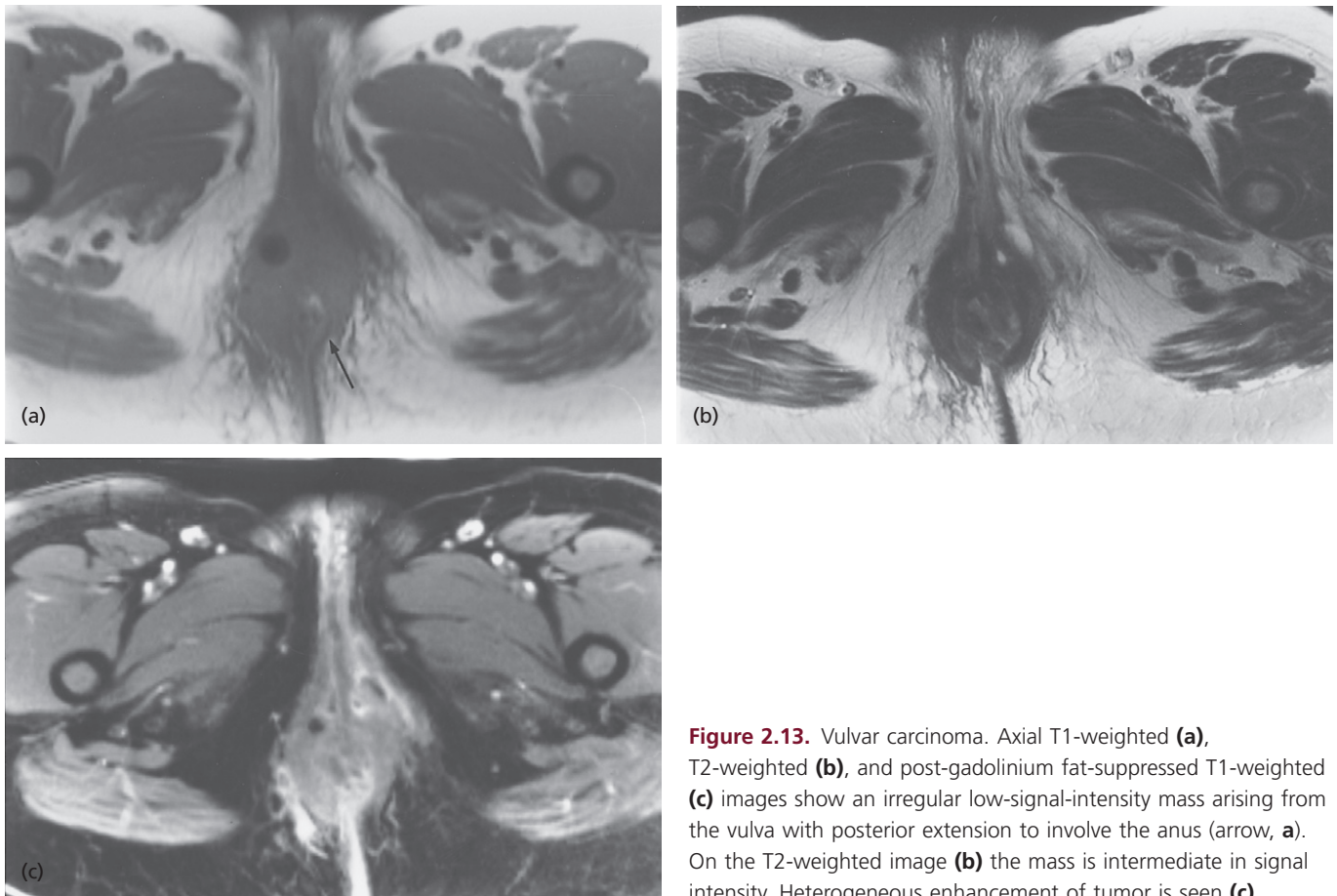


Figure 2.13. Vulvar carcinoma. Axial T1-weighted **(a)**, T2-weighted **(b)**, and post-gadolinium fat-suppressed T1-weighted **(c)** images show an irregular low-signal-intensity mass arising from the vulva with posterior extension to involve the anus (arrow, **a**). On the T2-weighted image **(b)** the mass is intermediate in signal intensity. Heterogeneous enhancement of tumor is seen **(c)**.